DOI: 10.63527/1607-8829-2026-1-17-32

O.H. Kulyk (https://orcid.org/0009-0001-2499-6813),
Y.V. Shmyhelskyi (https://orcid.org/0009-0004-3577-6877),
M.F. Pavlyuk (https://orcid.org/0000-0002-5663-2918),
I.V. Horichok (https://orcid.org/0000-0001-9748-3288)

Vasyl Stefanyk Carpathian National University, Ivano-Frankivsk, 76018, Ukraine

Corresponding author: I.V. Horichok, e-mail: *Ihor.Horichok@cnu.edu.ua*

Calculation of the Average Figure of Merit ZT_{avg} of Thermoelement Material Taking into Account its Temperature Profile

The paper analyzes the differences in the average values of the dimensionless thermoelectric figure of merit ZT_{avg} when averaging over the operating temperature range with and without taking into account the real temperature distribution along the legs. The temperature distribution along the thermoelements is calculated based on some low-temperature (based on Bi_2Te_3) and medium-temperature (based on PbTe) materials. The maximum efficiency η is estimated based on the dependence $\eta = f(ZT_{avg})$ for the considered materials and their series-connected combinations, as the basis for segment thermoelements.

Keywords: thermoelectric materials, thermal conductivity, thermoelectric figure of merit, efficiency.

Introduction

Thermoelectric converters, which directly convert thermal into electrical energy, are characterized by high reliability, compactness, and environmental friendliness, which makes them promising for a wide range of applications [1–3]. In modern conditions of increasing requirements for energy efficiency and rational use of resources, optimization of thermoelement parameters is of particular importance, which determines the efficiency of thermoelectric modules in different temperature ranges. Selection of optimal material characteristics and design parameters makes it possible to increase the conversion coefficient, reduce energy losses and ensure stable operation of the system under given conditions.

Citation: O.H. Kulyk, Y.V. Shmyhelskyi, M.F. Pavlyuk, I.V. Horichok (2026). Calculation of the Average Figure of Merit ZT_{avg} of Thermoelement Material Taking into Account its Temperature Profile. *Journal of Thermoelectricity*, (1), 17–32. https://doi.org/10.63527/1607-8829-2026-1-17-32

Received: 10.02.2026; Revised: 16.03.2026; Published: 31.03.2026

One of the most consistent methods for calculating the efficiency of converting thermal into electrical energy in a thermoelement is to solve a system of two differential equations describing the heat flow q and electric current j [4]:

$$\mathrm{div}\,\mathrm{q} = 0, \mathrm{div}\,\mathrm{j} = 0. \quad (1)$$

To obtain correct numerical values of the efficiency, it is necessary to take into account many factors, in particular, the temperature dependences of the Seebeck coefficient $S(T)$, the specific electrical conductivity $\sigma(T)$ and the thermal conductivity coefficient $k(T)$, the electrical resistances of the contact and transient layers, etc. This problem is relatively laborious and is usually solved using numerical methods and mathematical or physical application programs, such as COMSOL [4]. However, for the case of optimal conditions that provide the maximum efficiency of the thermoelement, this value (efficiency) can be estimated by a relatively simple analytical dependence [5]:

$$\eta = \frac{T_h - T_c}{T_h} \frac{\sqrt{ZT_{avg}+1}-1}{\sqrt{ZT_{avg}+1}+\frac{T_c}{T_h}}. \quad (2)$$

Here, T_h, T_c are the temperatures of the hot and cold ends of the thermoelement, ZT_{avg} is the average value of the dimensionless figure of merit ZT in the temperature range (T_c–T_h) [5]:

$$ZT = \frac{S^2\sigma}{\kappa}T. \quad (3)$$

Then [5]

$$ZT_{avg} = \frac{1}{T_h - T_c}\int_{T_c}^{T_h}\frac{S^2\sigma}{\kappa}T \cdot \mathrm{d}T. \quad (4)$$

Averaging the ZT value according to (4) will be correct in the case of a linear temperature distribution in a thermoelement. However, it is known that this distribution, although usually close to linear, is somewhat different from that in the case of a real thermoelement. The task of this work was to calculate the real temperature distribution in a thermoelement and to evaluate the influence of the ZT averaging method on the numerical efficiency values calculated using this method by example of several of the most effective low- and medium-temperature thermoelectric materials known today.

Properties and methods of obtaining some effective thermoelectric materials based on $A^5{}_2B^6{}_3$ and A^4B^6 compounds

Compounds $A^5{}_2B^6{}_3$ and A^4B^6 are among the most common materials used to create thermoelectric converters. This is due to many factors. First of all, as is known, these materials are characterized by a set of fundamental characteristics that contribute to the possibility of achieving high figures of merit. This, in particular, is the multi-valley energy spectrum of carriers and their small effective masses, high carrier mobilities and relatively low values of the thermal conductivity coefficient. In addition, these materials can usually be obtained with both n- and p-type conductivity, and the solubility of many impurities in these materials is quite high, which

contributes to the possibility of optimizing the chemical potential of carriers in materials and reducing the thermal conductivity coefficient, especially when creating solid solutions. Another important advantage of these materials is a relatively simple, well-studied production technique.

To date, the most proven method for producing low-temperature thermoelectric materials based on Bi_2Te_3 involves creating solid solutions of $Bi_2Te_{2,7}Se_{0,3}$ to obtain n-type conductivity legs and $Bi_{0,5}Sb_{1,5}Te_3$ to obtain p-type conductivity legs. These solution compositions provide relatively low values of the lattice components of the thermal conductivity coefficient, and additional doping optimizes the chemical potential of the carriers to achieve maximum *ZT* values.In particular, the possibility of increasing the figure of merit of the $Bi_2Te_{2.7}Se_{0.3}$ solid solution by doping with iodine was demonstrated in [6]. High-purity components Bi, Te, Se, and I were used to synthesize the chemical compounds $Bi_2Te_{2.7-x}Se_{0.3}I_x$. They were fused in pre-cleaned quartz ampoules at a temperature of 1000 K. The ampoules with the charge were evacuated at a pressure of 10^{-4} mbar. The synthesis was carried out in an oscillating furnace, which could change the angle in the range of ±30° with a period of 15 s, which ensured forced mixing of the components. At a temperature of 1000 K, the ampoule was removed from the furnace and quenched in cold water. The resulting material was ground in a planetary ball mill. The powder was then pressed in a protective atmosphere at room temperature into pellets 20 mm in diameter and 5 mm thick under a pressure of 1 GPa. These pellets were then compacted using spark plasma sintering under an axial pressure of 60 MPa in an argon atmosphere. The sintering temperature was 673 K, and the process lasted 20 minutes. The heating/cooling rate was 50 K/min.

The Seebeck coefficient of the materials studied in [6] is characterized by a non-monotonic temperature dependence, with a maximum, the coordinates of which depended on the iodine content. The temperature dependence of the thermal conductivity coefficient is also non-monotonic, with a minimum around 350–400 K. The specific electrical conductivity decreases with increasing *T*. The *ZT*(*T*) dependences are characterized by a maximum around 400 K. The highest values of $ZT \approx 1.2$ are observed for the composition $Bi_2Te_{2.695}Se_{0.3}I_{0.005}$ at 415 K. For a material without iodine impurity, the maximum value of *ZT* is ≈ 1.1 at 380 K.

In [7], the possibility of increasing the thermoelectric efficiency of the $Bi_2Te_{2.7}Se_{0.3}$ solid solution by adding a nanodispersed Cu_2Te additive to the pre-synthesized and ground material during the pressing stage was investigated. The $Bi_2Te_{2.7}Se_{0.3}$ array was synthesized using a fusion method followed by quenching. Pure elements (Bi, Te, Se with a purity of 99.999 %) were mixed in the required proportions, evacuated, and heated to a temperature of 1000 K for 6 hours. Following that, the ampoules were rapidly cooled in water. The obtained ingots were ground in a ball mill to a powder state. Cu_2Te nanoparticles were synthesized separately by chemical reduction method. For this, tellurium was dissolved in an aqueous solution of $NaBH_4$ after which an aqueous solution of $CuCl_2 \cdot H_2O$ was added. After the reaction was completed, the precipitate was centrifuged and washed with ethanol. The obtained nanoparticles had a size of 20–50 nm. Next, $Bi_2Te_{2.7}Se_{0.3}$ powder was mixed with Cu_2Te nanoparticles in ethanol, this mixture was dried in vacuum and sintered by spark plasma sintering (SPS) at a temperature of 773 K under a pressure of 60 MPa for 3 minutes.

According to the results of measuring thermoelectric parameters obtained in [7], the introduction of Cu_2Te nanoparticles contributes to a significant decrease in lattice thermal conductivity due to the effective scattering of phonons. The best effect was observed with the introduction of 0.4 % Cu_2Te. At higher concentrations, the particles begin to stick together, which worsens phonon scattering. The authors of [7] managed to achieve a maximum figure of merit $ZT \approx 0.75$ at a temperature of 374 K. This is 15 % better than that of the original material without the addition of Cu_2Te ($ZT \approx 0.65$ at 425 K), however, much less than in the case of iodine doping described in [6].

Low-temperature p-type materials based on $Bi_{0,5}Sb_{1,5}Te_3$, even without doping, exhibit higher ZT values than n-type materials. Thus, according to [6], for an undoped solid solution of the $Bi_{0.5}Sb_{1.5}Te_3$ composition, the maximum value of 0.95 was achieved at 330 K. The production technique is similar to that described above for the n-type material $Bi_2Te_{2.7}Se_{0.3}$ from the same work. The nature of the temperature dependences of S, σ, and k is also similar to those of n-type materials.

Adding lead to the solution does not lead to a significant improvement in the *ZT* value [6]. On the other hand, when copper is added, the *ZT* value can be increased to values of ≈ 1.2 [8]. The authors of this work used an original method of dispersing the synthesized solid solution of $Cu_{0.07}Bi_{0.5}Sb_{1.5}Te_3$ using a water jet at the crystallization stage. The obtained powders were sintered by hot pressing at 490 °C for 30 minutes under a pressure of 50 MPa. The nature of the temperature dependences of $S(T)$, $\sigma(T)$ and $k(T)$ is also similar to the other materials described above.

The most effective medium-temperature thermoelectric materials of n-type conductivity are usually obtained based on solid solutions of A^4B^6 with a predominant PbTe content, and p-type ones with a predominant GeTe content.

To obtain solid solutions based on n-type lead telluride and optimize the carrier concentration, doping with iodine is most often carried out. With its use, it is possible to achieve *ZT* values that correspond to the estimates of the maximum figure of merit for n-PbTe [9], if the phonon subsystem is not additionally affected. Thus, in [10] and [11], almost identical maximum values of $ZT \approx 1.4$ for PbTe:I were achieved. In both works, the material was obtained by fusing the components in evacuated quartz ampoules. The synthesis was carried out at 1273 K for 6 hours, after which the ingots were quenched in water. After synthesis, additional annealing was carried out at 973 K for 48 hours. After annealing, the ingots were crushed manually. The resulting powder was compacted by induction hot pressing at a temperature of 823 K for 1 hour under a pressure of 44 MPa.

At relatively high iodine concentrations in PbTe (according to [5] – from 0.0007 at. parts), the $S(T)$ dependences are monotonically increasing, and σ(T) – monotonically decreasing functions. The $k(T)$ dependences are monotonically decreasing functions starting from a concentration of 0.002 at. parts, while at lower concentrations, due to the manifestation of bipolar conductivity, this dependence is characterized by a minimum around 600–700 K. The highest thermoelectric figure of merit *ZT* in [5] was achieved for the composition of 0.0028 at. parts, although ZT_{avg} is equally high for compositions with a slightly lower iodine content

(0.0007, 0.0012 and 0.0020 at. parts). The authors of [5] emphasize that the material $PbTe_{0.9993}I_{0.0007}$ has very stable and reproducible properties.

In [12], the advantages of simultaneous doping with iodine and indium are presented, which are associated with the creation of an energy subband by the In impurity and the peculiarities of its filling with electrons due to the presence of an iodine impurity in the crystal. However, the *ZT* values obtained by the authors are approximately the same as in [10].

For p-type materials based on A^4B^6 compounds, some of the highest *ZT* values were obtained for $Ge_{1-x-y}Pb_xBi_yTe$ solid solutions. In particular, the positive effect of Bi and Pb on the properties of GeTe was demonstrated in [13]. Pure (99.999 %) Ge, Te, and Bi elements were used for the synthesis of the material. Stoichiometrically correct amounts of the starting elements were loaded into a quartz ampoule, which was hermetically sealed at a pressure of $\approx 2 \cdot 10^{-3}$ mbar. The ampoules were placed in a melting furnace and slowly heated to 1223K for 8 hours, then held at this temperature for 10 hours and gradually cooled to room temperature for approximately 6 hours. The resulting alloys were manually crushed and consolidated by spark plasma sintering at a temperature of 750 K for 5 minutes and an axial pressure of about 60 MPa. The heating rate was ~ 80 K/min. The resulting samples, characterized by a density of > 98%, were cut and polished for thermoelectric measurements.

Studies have shown that due to the substitution of Ge atoms by Bi atoms, the hole concentration decreases, which brings the Fermi level position closer to the optimal one. This allows the material to demonstrate a high dimensionless thermoelectric figure of merit *ZT*, which reaches $ZT \approx 2$ at 800 K. The temperature dependence of the Seebeck coefficient was characterized by a maximum at 750 K. While the specific electrical conductivity and thermal conductivity in the range 300–800 K are monotonically decreasing functions.

In [14], with the simultaneous introduction of both bismuth and lead, it was possible to achieve *ZT* values > 2. Pure elements Ge, Pb, Bi, and Te were used to synthesize thermoelectric alloys $Ge_{0.87}Pb_{0.13}Bi_{0.1}Te_{1.15}$. The components were loaded into quartz ampoules, which were hermetically sealed at a pressure of approximately 10^{-5} torr. Melting was carried out in an oscillatory furnace at a temperature of 1273 K for an hour, which ensured effective mixing of the melt and homogeneity of the liquid phase. After melting, the ampoules were quickly cooled in water to preserve the formed crystal structure and reduce the risk of the formation of unwanted phases. The resulting ingot was manually ground to powder using an agate mortar and pestle, ensuring a uniform particle size. Then, the powder was compacted by spark plasma sintering at a temperature of 823 K under a pressure of 25 MPa for 60 min.

In the obtained samples, a significant decrease in lattice thermal conductivity (up to 50 %) is observed. The combination of low thermal conductivity and optimal carrier concentration provides a high thermoelectric figure of merit *ZT*, which reaches values of ≈ 2.1 for the composition $Ge_{0.87}Pb_{0.13}Bi_{0.1}Te_{1.15}$.

Among other p-type materials based on A^4B^6compounds, mention should be made, in particular, of the PbTe–PbSe–PbS [15], [16] and PbTe–SrTe [17] solid solutions additionally doped with Na. In particular, in [16] $ZT = 2.24$ was obtained for the $PbTe_{0.75}PbSe_{0.20}PbS_{0.05}$ 800 K composition. To synthesize this solution, the authors used pre-obtained PbSe and PbS,

which made it possible to avoid significant losses of selenium and sulfur during melting. High-purity elements Pb (99.999 %), Te (99.999 %) and Na (99.99 %) were added to them. All components were loaded into quartz ampoules with an internal carbon coating, evacuated (~ 10^{-4}torr), and hermetically sealed. The ampoules were then heated to 1100 °C, held for 10 hours, and quickly quenched in cold water. The resulting ingots were annealed at 500 °C for 72 hours, after which they were manually crushed and consolidated by hot pressing. Pressing was performed in a 12.7 mm diameter graphite mold at a pressure of 40 MPa, a temperature of 500 °C, and a vacuum for 1 hour.

For the specified composition, the Seebeck coefficient increases almost linearly with a rise in temperature. This behavior is explained by the authors by the increase in the energy selectivity of charge carrier transport, which is associated with the convergence of valence bands at high temperatures. The electrical conductivity of the alloy decreases with increasing temperature, which is typical for degenerate semiconductors. The thermal conductivity of the material also shows a decrease with a rise in temperature, which is due to the effective scattering of phonons, in particular due to significant disordering when tellurium is simultaneously replaced by both selenium and sulfur.

Calculation of ZT_{avg} and $T(x)$

Fig. 1 shows the $ZT(T)$ dependences for the above-discussed materials of n- and p-type conductivity, which, in particular, clearly demonstrate the temperature ranges of effective operation of different materials. Of all the dependences, it is worth paying attention to the atypical temperature dependence of the figure of merit for the p-$Ge_{0.87}Pb_{0.13}Bi_{0.1}Te_{1.15}$ solid solution studied in [14]. The achievement of $ZT \approx 2$ already at 600 K and the presence of a plateau at higher temperatures will determine the prospects of this composition for practical application. Other materials are characterized by $ZT(T)$ dependences typical for these compounds.

Based on the dependencies shown in Fig. 1, ZT_{avg} was calculated. For this purpose, the $ZT(T)$ dependencies given in the literature were digitized with a step of 5 K, and the average values were found as $ZT_{avg} = 1\frac{1}{N}\sum_{i=1}^{N} ZT(T_i)$. The lower T_c and upper T_h boundaries of the temperature ranges, together with the obtained average values of ZT_{avg} for n- and p-type materials, are presented in Table 1. The table also shows the maximum material efficiency η in the conversion of thermal energy into electrical energy, calculated based on equation (2).

Here it is worth paying attention to the significant influence of the temperature T_h and, especially, T_c on the result of the calculation of η. The upper limit of the material's operation T_h is determined either by the value of the thermoelectric efficiency or by the thermal stability of its properties. At the same time, the lower limit T_c is usually determined by practical methods of cooling the cold end of the thermoelement. Usually it is estimated to be no higher than 100 °C, although theoretically it can be lower than 0 °C. And here it is important that with the same ZT_{avg} and ΔT, the efficiency will increase with decreasing T_c (Fig. 2).

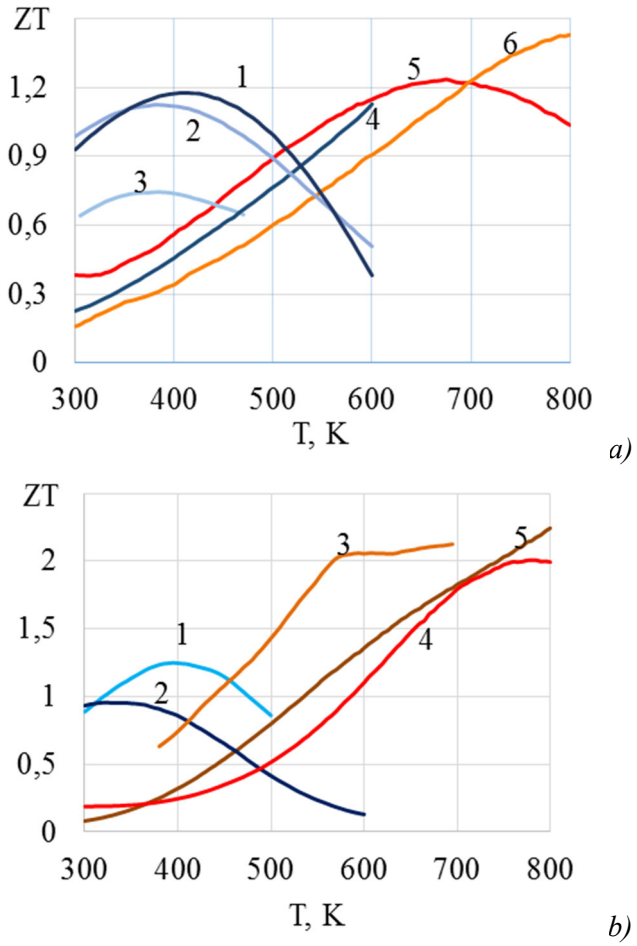

Fig. 1. Temperature dependence of the dimensionless thermoelectric figure of merit ZT for some materials of n-type (a) and p-type (b) conductivity. a: 1 – $Bi_2Te_{2.695}Se_{0.3}I_{0.005}$ [6], 2 – $Bi_2Te_{2.7}Se_{0.3}$ [6], 3 – $Bi_2Te_{2.7}Se_{0.3}$ + nano Cu_2Te [7], 4 – PbTe:I ($n = 1.8\times10^{19}$) [11], 5 – $PbTe_{0,998}I_{0,002}$ [10], 6 – $PbTe_{0.9993}I_{0.0007}$ [10]; b: 1 – $Cu_{0.07}Bi_{0.5}Sb_{1.5}Te_3$ [8], 2 – $Bi_{0.5}Sb_{1.5}Te_3$ [6], 3 – $Ge_{0.87}Pb_{0.13}Bi_{0.1}Te_{1.15}$ [14], 4 – $Ge_{0.96}Bi_{0.04}Te$ [13], 5 – $PbTe_{0.75}PbSe_{0.20}PbS_{0.05}$ [16]

Table 1

The calculated values of ZT_{avg} and efficiency for materials of n- and p-type conductivity

	T_h, K	T_c, K	ZT_{avg}	η, %
$Bi_2Te_{2.7}Se_{0.3}$	600	300	0.94	10.3
$Bi_2Te_{2.695}Se_{0.3}I_{0.005}$	600	300	0.97	10.6
$PbTe_{0.9993}I_{0.0007}$	800	300	0.91	13.6
$PbTe_{0.998}I_{0.002}$	800	300	0. 78	12.2
$Bi_{0.5}Sb_{1.5}Te_3$	600	300	0.61	7.57
$Cu_{0.07}Bi_{0.5}Sb_{1.5}Te_3$	500	300	1.11	8.8
$Ge_{0.87}Pb_{0.13}Bi_{0.1}Te_{1.15}$	695	380	1.59	12.8
$Ge_{0.96}Bi_{0.04}Te$	800	300	0.95	14
$PbTe_{0.75}PbSe_{0.20}PbS_{0.05}$	800	300	1.09	15.3

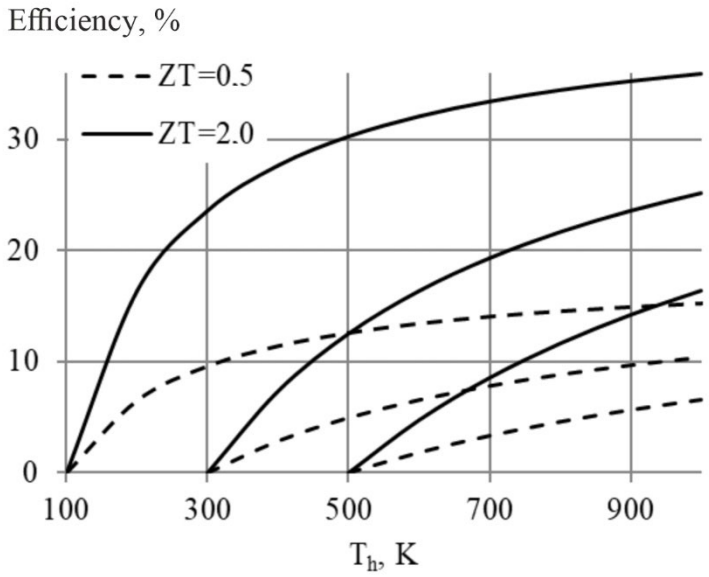

Fig. 2. Dependence of the efficiency on the hot end temperature at the cold end temperatures of 100 K, 300 K and 500 K for ZT_{avg} = 0.5 (dashed curve) and ZT_{avg} = 2.0 (solid curve)

A more correct result in estimating ZT_{avg}, and hence the efficiency, can be achieved if averaging is performed not over the temperature range, but over the real temperature distribution along the thermoelement. It is known that such a distribution is somewhat different from linear, especially when current flows through it, due to the release of the Joule heat and the release (if the direction of the current coincides with the direction of the heat flow) or absorption (if they are opposite) of the Thomson heat. Fig. 3 shows the calculated temperature distributions along the thermoelement in the form of a rectangular parallelepiped at fixed temperature values at its ends for some materials from Table 1. The calculation was performed based on the equation [18]:

$$\frac{\mathrm{d}}{\mathrm{d}x}\left(k\frac{\mathrm{d}T}{\mathrm{d}x}\right)+\frac{j^2}{\sigma}-jT\frac{\mathrm{d}S}{\mathrm{d}T}\frac{\mathrm{d}T}{\mathrm{d}x}=0 \qquad (5)$$

with the boundary conditions $T(0) = T_h$, $T(L) = T_c$, and $j = I \cdot L/A$, where I is the current in the sample, L is the length of the sample, and A is the cross-sectional area of the sample. Here, the second term takes into account the Joule heat, and the third – the Thomson heat. Heat losses due to the lateral faces were assumed to be absent. It was taken into account that the direction of the current through the sample coincides with the direction of the heat flow. The size of the thermoelement: L = 1 cm for medium-temperature materials and L = 0.4 cm for low-temperature materials, $A = 0.5 \cdot 0.5$ см^2.

The dashed line in Fig. 3 shows the dependence $T(x)$ for the case when the thermal conductivity coefficient is strictly determined by the dependence $k = V/T$ at current I = 0 A. It is important that in this case $T(x)$ does not depend on the value of V:

$$T = T_h\left(\frac{T_h}{T_c}\right)^{-x/L}. \qquad (6)$$

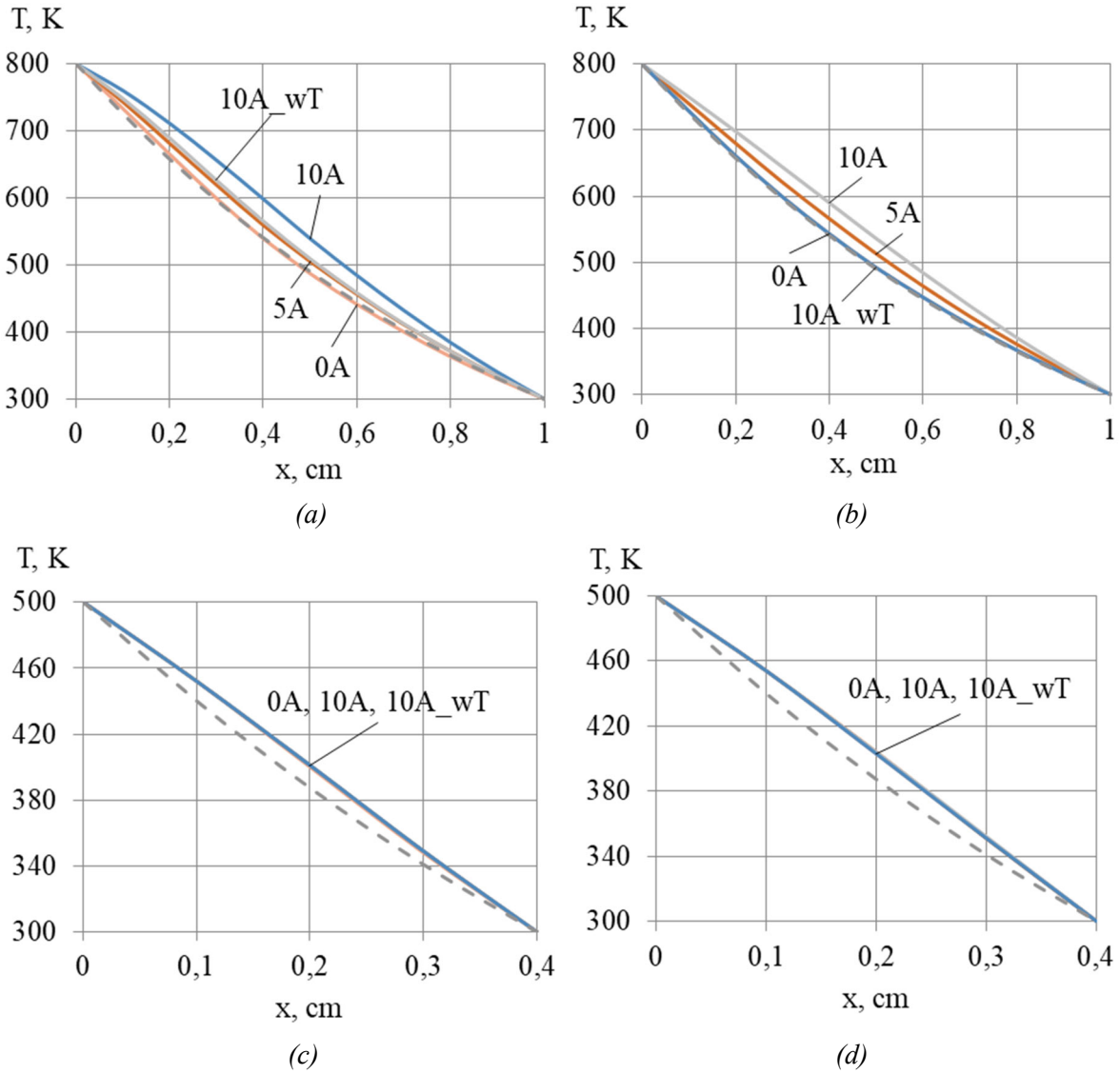

Fig. 3. Temperature distribution along the samples $PbTe_{0.9997}I_{0.0007}$ (a), PbTe-PbSe-PbS:Na (b), $Bi_2Te_{2.695}Se_{0.3}I_{0.005}$ (c), $Cu_{0.07}Bi_{0.5}Sb_{1.5}Te_3$ (d) at fixed temperatures of the hot (800 K or 500 K) and cold (300 K) ends

Fig. 4 shows the experimental dependences of thermoelectric parameters from works [6–17]. It is seen that for n- and p-type conductivity of materials based on PbTe only in the region of 700–800 K, due to the influence of the bipolar component, the dependence $k(T)$ differs from that close to $1/T$. Therefore, for compounds based on PbTe, the dependences $T(x)$ obtained from (6) practically coincide with the real ones obtained on the basis of formula (5). At the same time, for compounds BiTeSe and BiSbTe, a significant difference is observed.

The passage of current leads to a change in temperature along the length of the sample. According to literature data, the optimal current values in thermoelements, at which maximum efficiency is achieved, usually do not exceed 5 A. According to the results of the calculation, at such a current the temperature at the middle of the sample for the analyzed materials based on A^4B^6compounds increases by approximately 20 K. At 10 A this value is approximately 40 K for p-PbTe-PbSe-PbS:Na and approximately 50 K for n-PbTe:I. Moreover, for an n-type

material the contribution of the Thomson heat is commensurate with the Joule heat, and for the p-type it is significantly greater. Obviously, this is due to a sharper increase in the Seebeck coefficient with increasing T (Fig. 4, *a*), since the Thomson coefficient is proportional to d*S*/d*T* ($\tau = T \cdot dS/dT$ [19]).

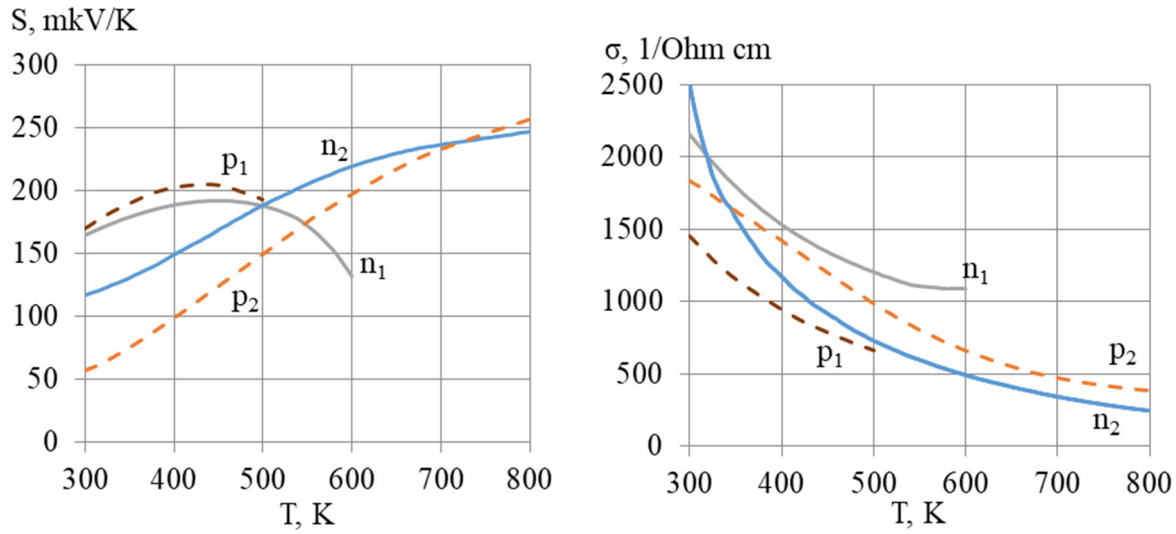

a)

b)

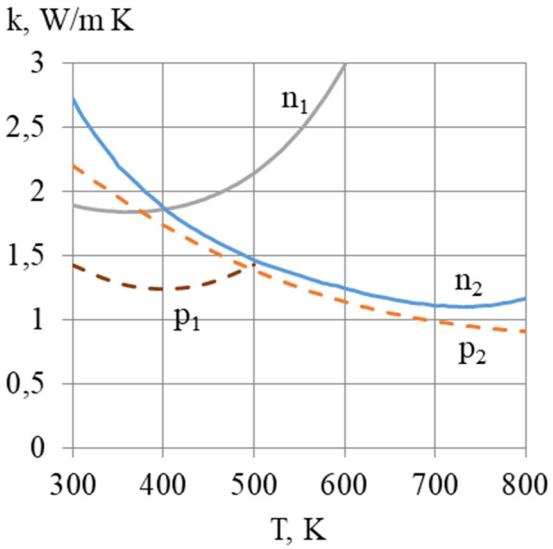

c)

Fig. 4. Temperature dependences of the main thermoelectric parameters (a – the Seebeck coefficient S, b – specific electric conductivity σ, c –thermal conductivity coefficient k) for materials $Bi_2Te_{2.695}Se_{0.3}I_{0.005}$ (n_1) [6], $PbTe_{0.9997}I_{0.0007}$ (n_2) [10], $Cu_{0.07}Bi_{0.5}Sb_{1.5}Te_3$ (p_1) [8], PbTe-PbSe-PbS:Na (p_2) [16]

For low-temperature materials, the change in $T(x)$ due to the release of the Joule and Thomson heat is only a few tenths of a Kelvin. This is primarily due to the smaller difference in operating temperatures at the ends, and secondly, to the smaller sample size (length). The specific temperature difference was chosen based on the standard operating range for these materials, and the smaller sample size for low-temperature materials was chosen to maintain

the same temperature difference per unit length for both medium-temperature and low-temperature materials – 500 K/cm. If we attempt to calculate the $T(x)$ distribution for low-temperature materials in the range of 300–800 K, the heat contribution increases significantly, primarily the Joule heat, since at high temperatures, the specific electrical conductivity of Bi_2Te_3-based materials is lower than that of PbTe-based materials, and the $T(x)$ dependences will be similar. However, it is clear that this range does not correspond to the actual performance capabilities of the material.

Table 2 shows the efficiency values calculated as averages over the temperature distribution for n- and p-type PbTe thermoelements. We see that the changes in the numerical efficiency values when changing the ZT_{avg} calculation method are up to 2 percent. If we analyze the relative changes, this is approximately 10 %. For low-temperature materials, the effects will be qualitatively similar, but the numerical changes will not exceed a few tenths of a percent.

Table 2

The calculated values of ZT_{avg} and efficiency taking into account the temperature distribution along the sample T(x) for two materials of n- and p-type conductivity at T_c = 300 K, T_h = 800 K

	n-$PbTe_{0.9993}I_{0.0007}$		p-$PbTe_{0.75}PbSe_{0.20}PbS_{0.05}$	
Type of dependence $T(x)$	ZT_{avg}	η, %	ZT_{avg}	η, %
Linear	0.91	13.6	1.10	15.4
According to expression (6)	0.83	12.8	0.93	13.8
Calculated from expression (5) at I = 5A	0.85	13.0	1.00	14.4

Estimation of η for segmented thermoelements based on A^4B^6 and $A^5{}_2B^6{}_3$

The use of segmented thermoelements, i.e. two materials of the same conductivity type connected in series, one exhibiting a higher thermoelectric figure of merit at lower temperatures and the other at higher temperatures, helps increase the average ZT_{avg} value over the entire operating range of 300–800 K, leading to increased efficiency. Segmentation thus compensates for the drop in figure of merit beyond temperature, matching the peak ZT values of individual materials and ensuring more efficient use of the temperature gradient. Solid solutions based on Bi_2Te_3 and PbTe compounds are frequently investigated as materials for the low-temperature and high-temperature segments of thermoelements, respectively. Literary examples of creating modules based on segmented thermoelements using the aforementioned materials confirm their technological compatibility and the absence of critical issues when combined within a single

leg, provided the contact temperature and connection technology are properly selected [4, 20–25].

Among the $ZT(T)$ dependences shown in Fig. 1, the materials n-$Bi_2Te_{2.695}Se_{0.3}I_{0.005}$ and n-$PbTe_{0.9997}I_{0.0007}$ for the n-type leg and $Cu_{0.07}Bi_{0.5}Sb_{1.5}Te_3$ and p-$PbTe_{0.75}PbSe_{0.20}PbS_{0.05}$:Na for the p-type leg were selected to assess the efficiency of the segmented leg. The temperature at which the $ZT(T)$ dependences for each of these pairs intersect can be used to determine the leg sizes, using the $T(x)$ dependences calculated above. A more correct value of this temperature, which takes into account the condition of minimizing power losses in sections with high resistance and low thermo-emf [4], is determined by the point of intersection of the dependences

$$s(T) = \frac{Z(T)}{(1+\sqrt{1+Z(T)\cdot T})\cdot S(T)} \tag{7}$$

for each pair of n- and p-type materials. The contact temperature of the low-temperature and high-temperature segments thus determined is 525 K for n-type materials and 475 K for p-type materials. These values differ slightly from those obtained from the $ZT(T)$ cross-section in Fig. 1: 510 K for n-type materials and 505 K for p-type materials.

Using these temperature values, ZT_{avg} for the segmented leg was calculated as the arithmetic mean in the temperature range 300–800 K:

$$ZT_{avg} = \frac{1}{N}\sum_{i=1}^{N} ZT_{segm}(T_i). \tag{8}$$

Here

$$ZT_{segm}(T) = \begin{cases} ZT_L(T), & T \le T_{cont} \\ ZT_H(T), & T > T_{cont} \end{cases}. \tag{9}$$

For the segmented n-type leg, the average figure of merit $ZT^n_{avg} = 1.12$ was obtained, and the corresponding efficiency value is 15.55 %. For the segmented p-type leg, $ZT^n_{avg} = 1.12$ was obtained, and the efficiency is 17.77 %. The efficiency increase of the segmented legs compared to the leg made only of PbTe-based material is about 2 %. In relative units, this is about 15 %. Since the calculation does not take into account the resistance of contacts and transient layers, the obtained values are somewhat overestimated. Comparing with the literature data obtained on the basis of sequential calculation based on the heat flow and charge equations, we can conclude that the overestimation is 3–5 %. However, the relative estimate of the increase in the value of η is fully consistent with the literature data. If we take into account the real temperature distribution in the calculations using expressions (8–9), we can achieve better agreement with the absolute values of η for the segmented leg.

Regarding the relative segment size estimation, an analysis of Fig. 3 shows that a temperature of 500 K for PbTe-based thermocouples is reached at a distance of 0.5–0.6 mm from the hot end. Of course, this estimate of the hot segment size is inaccurate, as it doesn't take into account the heat flow disturbance near the contact between the two segments. However,

given that the thermoelement does not always operate under optimal conditions, this approximation may be sufficient for a preliminary semi-quantitative assessment.

It is worth noting that to achieve maximum efficiency of thermoelectric modules, the cross-sectional area of the n- and p-type legs must satisfy the condition [14]

$$\frac{A_n}{A_p} = \sqrt{\frac{\sigma_p \cdot \kappa_p}{\sigma_n \cdot \kappa_n}}. \tag{10}$$

In our case, this ratio was calculated as

$$\frac{A_n}{A_p} = \left(\sum_{T_c}^{T_h} \sqrt{\frac{\sigma_p(T) \cdot \kappa_p(T)}{\sigma_n(T) \cdot \kappa_n(T)}} \Delta T \right) / (T_h - T_c). \tag{11}$$

For the selected combination of materials, the obtained optimal ratio of the cross-sectional areas of the legs is $A_n/A_p \approx 0.92$, which is consistent with the literature data for similar materials.

Conclusions

The temperature profile along thermoelements based on A^4B^6 and $A^5{}_2B^6{}_3$ materials at fixed temperatures of its ends was calculated and the effect of nonlinearity $T(x)$ on the average value of the dimensionless thermoelectric figure of merit ZT_{avg} and the efficiency determined on its basis was investigated.

It has been established that when calculating ZT_{avg} by averaging ZT not in a given temperature range, but taking into account the real temperature distribution along the sample, the obtained values will differ by up to 10 %, and the efficiency values calculated on their basis will differ by up to 2 %.

It is shown that using the formula for the maximum efficiency of a thermoelement, it is possible to correctly estimate the increment of this value for a segmented thermoelement, while the absolute values are overestimated by several percent.

Authors' information

O.H. Kulyk – Postgraduate student, Department of Physics and Astronomy, Vasyl Stefanyk Carpathian National University.
Y.V. Shmyhelskyi – Postgraduate student, Department of Physics and Astronomy, Vasyl Stefanyk Carpathian National University.
M.F. Pavlyuk – Candidate of Physical and Mathematical Sciences, Associate Professor, Associate Professor of the Department of Computer Engineering and Electronics, Vasyl Stefanyk Carpathian National University.
I.V. Horichok – Doctor of Physics and Mathematics, Professor, Professor of the Department of Physics and Astronomy, Vasyl Stefanyk Carpathian National University.

References

1. Zoui, M.A., Bentouba, S., Stocholm, J.G., Bourouis, M. (2020). A review on thermoelectric generators: Progress and applications. *Energies*, 13, 3606. https://doi.org/10.3390/EN13143606
2. Chen, L., Liu, R., Shi, X. (2021) Thermoelectric Materials and Devices. *Amsterdam: Elsevier*. https://doi.org/10.1016/c2018-0-02472-x
3. Petsagkourakis, I., Tybrandt, K., Crispin, X., Ohkubo, I., Satoh, N., Mori, T. (2018). Thermoelectric materials and applications for energy harvesting power generation. *Science and Technology of Advanced Materials*. 19, 836-862. https://doi.org/10.1080/14686996.2018.1530938
4. Manyk T. O., Bilynskyi-Slotylo V.R. (2014). Calculation of segmented modules based on Bi_2Te_3 / PbTe for thermoelectric generators. Physics and Chemistry of the Solid State, 15, 2, 413–417.
5. Goldsmid H. J. (2010). Introduction to Thermoelectricity. *Heidelberg: Springer*, 2010.
6. Maksymuk, M., Dzundza, B., Matkivsky, O., Horichok, I., Shneck, R., Dashevsky, Z. (2022). Development of the high performance thermoelectric unicouple based on Bi_2Te_3 compounds. *Journal of Power Sources*, 530, 231301. https://doi.org/10.1016/j.jpowsour.2022.231301
7. Jung, Y.-J., Kim, H.-S., Won, J. H., Kim, M., Kang, M., Jang, E. Y., Binh, N. V., Kim, S.-I., Moon, K.-S., Roh, J. W., Nam, W. H., Koo, S.-M., Oh, J.-M., Cho, J. Y., Shin, W. H. (2022). Thermoelectric properties of Cu_2Te nanoparticle incorporated n-type $Bi_2Te_{2.7}Se_{0.3}$. *Materials*, 15, 6, 2284. https://www.mdpi.com/1996-1944/15/6/2284
8. Madavali, B., Sharief, P., Park, K.-T., Song, G., Back, S.-Y., Rhyee, J.-S., Hong, S.-J. (2021). Development of high-performance thermoelectric materials by microstructure control of p-type BiSbTe based alloys fabricated by water atomization. *Materials*, 14, 17, 4870.
9. Khshanovska, O., Parashchuk, T., Horichok, I. (2023). Estimating the upper limit of the thermoelectric figure of merit in n- and p-type PbTe. *Materials Science in Semiconductor Processing*, 160, 107428. https://doi.org/10.1016/j.mssp.2023.107428
10. LaLonde, A. D., Pei, Y., Snyder, G. J. (2011). Reevaluation of $PbTe_{1-x}I_x$ as high-performance n-type thermoelectric material. *Energy & Environmental Science*, 4, 6, 2090. http://dx.doi.org/10.1039/c1ee01314a
11. Pei, Y., LaLonde, A. D., Wang, H., Snyder, G. J. (2012). Low effective mass leading to high thermoelectric performance. *Energy & Environmental Science*, 2012, 5, 7, 7963. http://dx.doi.org/10.1039/c2ee21536e
12. Parashchuk, T. Defect state engineering in chalcogenide materials for efficient energy conversion // XX International Freik conference on physics and technology of thin films and nanosystems. Materials. Ivano-Frankivsk, October 06-10, 2025. p.131.
13. Dashevsky, Z., Horichok, I., Maksymuk, M., Muchtar, A. R., Srinivasan, B., Mori, T. (2022). Feasibility of high performance in p-type $Ge_{1-x}Bi_xTe$ materials for thermoelectric modules. *Journal of the American Ceramic Society*, 105, 6, 4500–4511.

http://dx.doi.org/10.1111/jace.18371.

14. Gelbstein, Y., Davidow, J. (2014) Highly efficient functional $Ge_xPb_{1-x}Te$ based thermoelectric alloys. *Physical Chemistry Chemical Physics*, 16, 37, 20120–20126. http://dx.doi.org/10.1039/c4cp02399d
15. Qin, B., Hu, X., Zhang, Y., Wu, H., Pennycook, J.St., and Zhao, L.-D. (2019). Comprehensive Investigation on the Thermoelectric Properties of p-Type PbTe-PbSe-PbS Alloys. *Advanced Electronic Materials*, 5, 12, 1900609. http://dx.doi.org/10.1002/aelm.201900609
16. Ginting, D., Lin, C.-C., Rhyee, J.-S. (2019). Synergetic approach for superior thermoelectric performance in PbTe–PbSe–PbS quaternary alloys and composites. *Energies*, 13, 1, 72. http://dx.doi.org/10.3390/en13010072
17. Biswas, K., He, J., Blum, I. D., Wu, C-I, Hogan, T. P., Seidman, D. N., Dravid, V. P., Kanatzidis, M. G. (2012). High-performance bulk thermoelectrics with all-scale hierarchical architectures. *Nature*, 489, 7416, 414–418. http://dx.doi.org/10.1038/nature11439
18. Pei J., Li L. L., Liu D. W., Zhang B. P., Xiao Y. & Li J. F. (2019). Development of integrated two-stage thermoelectric generators for large temperature difference. Sci China Tech Sci, 2019, 62, 1596–1604. https://doi.org/10.1007/s11431-019-9498-y
19. Anatychuk L.I. (1979). *Thermoelements and thermoelectric devices: Handbook*. Kyiv*: Naukova Dumka,* 676.
20. Ouyang, Z., Li D. (2016). Modelling of segmented high-performance thermoelectric generators with effects of thermal radiation, electrical and thermal contact resistances. *Scientific Reports*, 6, 1, 24123. http://dx.doi.org/10.1038/srep24123
21. Vikhor, L. N., Anatychuk, L. I. (2009). Generator modules of segmented thermoelements. *Energy Conversion and Management*, 50, 9, 2366–2372. http://dx.doi.org/10.1016/j.enconman.2009.05.020
22. Anatychuk, L. I., Vikhor, L. N., Strutynska, L. T., Termena, I. S. (2011). Segmented generator modules using Bi_2Te_3-based materials. *Journal of Electronic Materials*, 2011, 40, 5, 957-961. http://dx.doi.org/10.1007/s11664-010-1468-x
23. Shu, G., Ma, X., Tian, H., Yang, H., Chen, T., Li, X. (2018). Configuration optimization of the segmented modules in an exhaust-based thermoelectric generator for engine waste heat recovery. *Energy*, 160, 612-624. http://dx.doi.org/10.1016/j.energy.2018.06.175
24. Hong, M., Zheng, K., Lyv, W., Li, M., Qu, X., Sun, Q., Xu, S., Zou, J., Chen, Z.-G. (2020). Computer-aided design of high-efficiency GeTe-based thermoelectric devices. *Energy & Environmental Science*, 13, 6, 1856-1864. http://dx.doi.org/10.1039/d0ee01004a
25. Hung, L. T., Nong, N. V., Han, L., Bjork, R., Ngan, P. H., Holgate, T. C., Balke, B., Snyder, G. J., Linderoth, S., Pryds, N. (2015). Segmented thermoelectric oxide-based module for high-temperature waste heat harvesting. *Energy Technology*, 2015, 3, 11, 1143-1151. http://dx.doi.org/10.1002/ente.201500176

Кулик О.Г. (https://orcid.org/0009-0001-2499-6813),
Шмигельський Я.В. (https://orcid.org/0009-0004-3577-6877),
Павлюк М.Ф. (https://orcid.org/0000-0002-5663-2918),
Горічок І.В. (https://orcid.org/0000-0001-9748-3288)

Карпатський національний університет імені Василя Стефаника,
Івано-Франківськ, 76018, Україна

Розрахунок середнього значення добротності матеріалу термоелемента ZT_{avg} з врахуванням його температурного профілю

В роботі проаналізовано відмінності середніх значень безрозмірної термоелектричної добротності ZT_{avg} при усередненні в інтервалі робочих температур з врахуванням реального розподілу температур вздовж віток та не враховуючи його. Розраховано розподіл температури вздовж термоелементів на основі деяких низькотемпературних (на основі Bi_2Te_3) та середньотемпературних (на основі PbTe) матеріалів. Оцінено максимальний коефіцієнт корисної дії η на основі залежності $\eta = f(ZT_{avg})$ для розглянутих матеріалів та їх послідовно з'єднаних комбінацій, як основи для сегментних термоелементів.

Ключові слова: термоелектричні матеріали, теплопровідність, термоелектрична добротність, коефіцієнт корисної дії.